CrossMark

ORIGINAL ARTICLE

IC design of driving circuit of MEMS microrobot using pulse-type hardware neuron model

Yuki Ishihara[1] · Yuka Naito[1] · Kazuaki Maezumi[1] · Yuki Okane[1] · Hirozumi Oku[1] ·
Masaki Tatani[1] · Minami Takato[1] · Ken Saito[1] · Fumio Uchikoba[1]

Abstract This paper presented a driving circuit which can output a driving waveform of the piezoelectric element impact-type actuator. The piezoelectric element impact-type actuator generates the rotational movement which is necessary to move the legs of the micro electro mechanical systems (MEMS) microrobot. The MEMS microrobot is made from silicon wafers fabricated by micro fabrication technology. The size of the fabricated MEMS microrobot is 4.0 mm × 4.6 mm × 3.6 mm. The driving circuit consists of a bare chip IC of the pulse-type hardware neuron model (P-HNM) and a peripheral circuit. P-HNM is an electrical oscillating model which has the same basic features of biological neurons. Therefore, P-HNM can output the driving waveform of the piezoelectric element impact-type actuator using electrical oscillation as biological neuron. As a result, we showed that the driving circuit can output the driving waveform of the piezoelectric element impact-type actuator without using any software programs or analog digital converters.

Keywords Bare chip IC · MEMS · Microrobot · Piezoelectric element · Pulse-type hardware neuron model

✉ Ken Saito
  kensaito@eme.cst.nihon-u.ac.jp

[1] Nihon University, 7-24-1 Narashinodai, Funabashi-shi, Chiba 274-8501, Japan

1 Introduction

Microrobots have been studied in various fields such as miniature component assembly fields or microsurgery fields. However, further miniaturization and higher functionalization of microrobots are needed to make them play a more active role in those fields [1, 2]. Especially, to realize the further miniaturization, developments of a small size actuator, an energy source and a controlling system have been required. However, conventional mechanical machining technology faces a problem with limitation in miniaturization. Therefore, some advanced studies use the micro electro mechanical systems (MEMS) technology for miniaturizing the microrobot [3, 4]. The miniaturization of the actuator has been usually researched in the conventional rotary actuator such as an electrostatic type motor [5] or an electromagnetic induction type motor [6]. However, there are disadvantages, such as the small amount of generative force or difficulty in miniaturization. Therefore, the actuator using the characteristic of the material itself has attracted attention [7].

Programmed control by a microcontroller has been a dominant system to control the microrobot. However, the programmed control cannot be processed appropriately under the specified environment with unexpected situations. The programmed control is effective for the repeating operation as one in a factory line. However, when a robot works in unusual environments such as inside the

human body, programmed control system is difficult to process. On the other hand, artificial neural networks imitating the biological information processing have possibilities in the advanced robot controlling. For example, several researches of construction of the artificial neural networks by modeling the biological neural networks have been reported [8–11]. However, using the mathematical neuron models in large scale artificial neural networks is difficult to process continuously because the computer simulation is limited by the computer performance, such as the processing speed and the memory capacity. In contrast, even if a circuit scale becomes large, the nonlinear operation of the hardware neuron model can perform at high speed and be processed continuously. Therefore, the construction of a hardware neuron model which can generate oscillatory patterns has been desired. The pulse-type hardware neuron model (P-HNM) proposed by Sekine can generate the oscillatory patterns using a simple electronic circuit [12, 13].

We are studying the MEMS microrobot system which can locomote without using any software programs or analog digital converters. Previously, we developed the MEMS microrobot generating the rotational movements of a rotor using the artificial muscle wire-type actuator [14–16]. The artificial muscle wire-type actuator can generate the movements of the MEMS microrobot with six legs. In addition, the pulse-type hardware neural networks can generate the driving waveform of the artificial muscle wire-type actuator. However, the size of the driving circuit is 8.5 mm square and it is too big to move the MEMS microrobot [17].

In this paper, we will discuss the small size driving circuit which can generate the driving waveform of the piezoelectric element impact-type actuator. We developed the driving circuit using P-HNM which consists of the bare chip IC of P-HNM using CMOS process and peripheral circuit. The driving circuit is 3.2 mm × 4.9 mm in size, which can be mounted on the MEMS microrobot.

2 MEMS microrobot

2.1 Component

A piezoelectric element impact-type MEMS microrobot is shown in Fig. 1. The MEMS microrobot consists of legs with a piezoelectric element impact-type actuator and a link mechanism. Each component is made from silicon wafers except the piezoelectric element and the shafts. The size of the fabricated robot is 4.0 mm in width, 4.6 mm in length, and 3.6 mm in height.

The component of a piezoelectric element impact-type actuator is shown in Fig. 2. The piezoelectric element
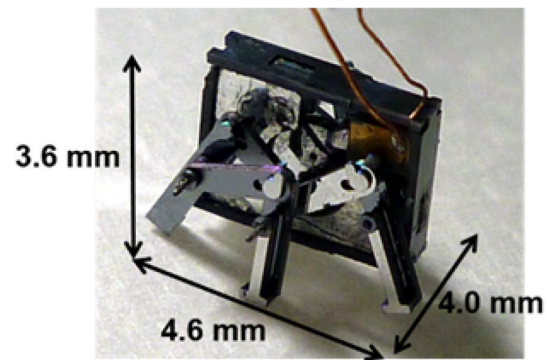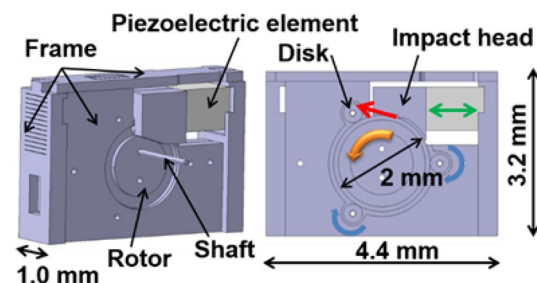
Fig. 1 Fabricated MEMS microrobot

Fig. 2 Components of the piezoelectric element impact-type actuator

Table 1 Specification of the piezoelectric element

Displacement	110 nm at 3 V
Capacitance	32 nF ± 20 %
Dielectric resistance	≥100 MΩ
Curie temperature	245 °C
Dimensions	0.9 mm × 0.9 mm × 1.0 mm

impact-type actuator consists of a frame, a rotor, a piezoelectric element and an impact head. Constructed actuator is measured in the size of 1.0 mm in width, 4.4 mm in length, and 3.2 mm in height. The specification of the piezoelectric element is shown in Table 1. The piezoelectric element can drive the actuator in low voltage.

2.2 Piezoelectric element impact-type actuator

Rotational motion of the rotor is generated by the voltage driving piezoelectric element. Firstly, driving waveform (pulse waveform) is inputted to a piezoelectric element. Secondly, the piezoelectric element vibrates in the displacement direction. Thirdly, impact head hit the rotor. Finally, rotational movement of the rotor makes the six legs move using a link mechanism. As a result, locomotion of the MEMS microrobot is realized.
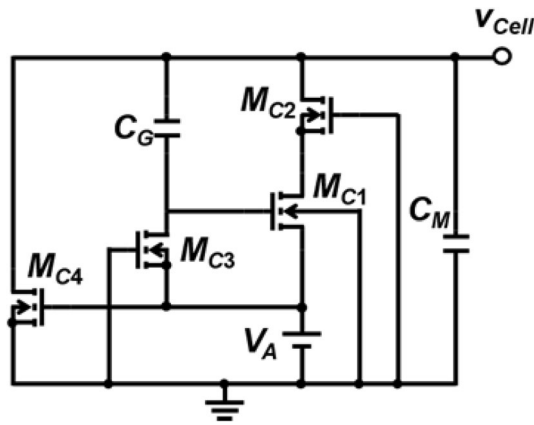
Fig. 3 The circuit diagram of the P-HNM

Fig. 4 The circuit diagram of current mirror circuit

3 Driving circuit

3.1 Pulse-type hardware neuron model

P-HNM can output the pulse waveform like living organisms. P-HNM has a characteristic of class II neuron [17] such as the Hodgkin-Huxley model [10] or Bonhoeffer-van der Pol model [11]. Therefore, P-HNM has the same basic features as biological neurons such as the threshold, the refractory period and the ability to generate the continuous pulse waveform. The basic circuit diagram of the P-HNM using the CMOS technology is shown in Fig. 3. The P-HNM consists of the capacitor C_G, the membrane capacitor C_M, and the MOSFETs M_{C1}, M_{C2}, M_{C3} and M_{C4}. The P-HNM is an electrical oscillating model which can output the pulse waveform using a negative resistance circuit, an equivalent inductor, and a capacitor. V_A is the power supply voltage of the P-HNM. v_{Cell} is the voltage between both ends of the capacitor C_M. The circuit parameters are $C_G = 150$ pF, $C_M = 15$ pF, M_{C1} and M_{C2}: $L = 5$ μm, $W = 50$ μm, M_{C3}: $L = 10$ μm, $W = 1$ μm, M_{C4}: $L = 10$ μm, $W = 3$ μm (where W is an effective channel width and L is an effective channel length of the MOSFETs. In the case where W/L become large, the current of the MOSFETs will increase).

The output pulse waveform of the P-HNM is inputted to the peripheral circuitry through a current mirror circuit for the purpose of current amplification and impedance adjustment. The circuit diagram of the current mirror circuit using CMOS technology is shown in Fig. 4. In Fig. 4, V_{DD} is the power supply voltage of the current mirror circuit and i_{out} is the output current of the current mirror circuit. Each circuit parameters are as follows: M_1: $L = 1.5$ μm, $W = 60$ μm, M_2: $L = 10$ μm, $W = 10$ μm, M_3: $L = 1.5$ μm, $W = 100$ μm.
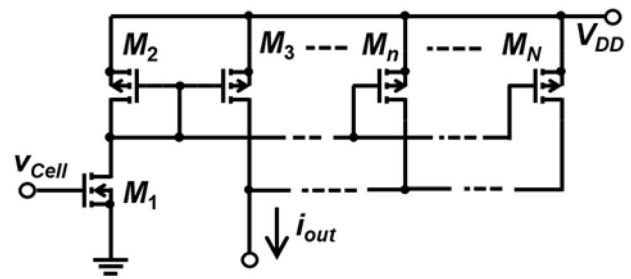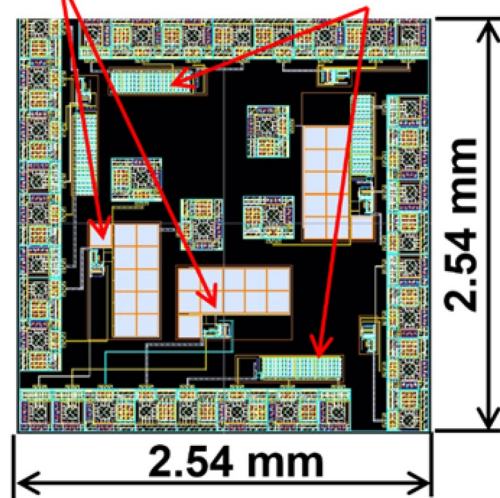

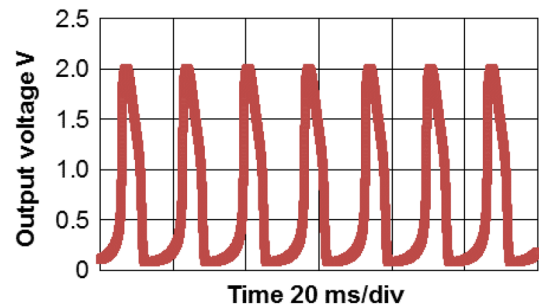**Fig. 5** Layout pattern of the IC chip

Fig. 6 Example of the output pulse waveform of the P-HNM (simulation result)

Figure 5 shows the example of the layout pattern of the constructed IC chip. The design rule of the IC chip is the 4 metal 2 poly CMOS 0.35 μm rule. In this layout, we construct P-HNMs and current mirror circuits. The IC chip is 2.54 mm square in size.
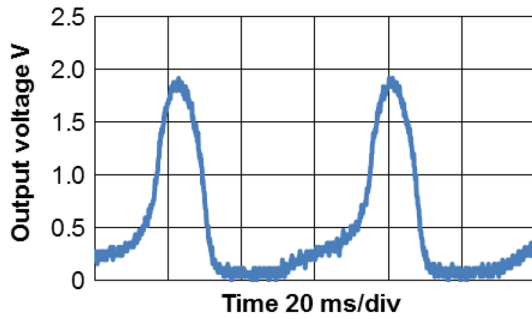
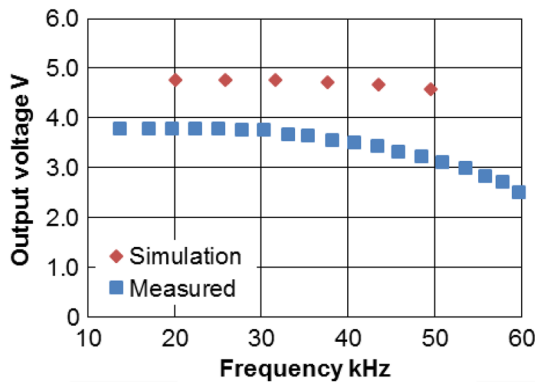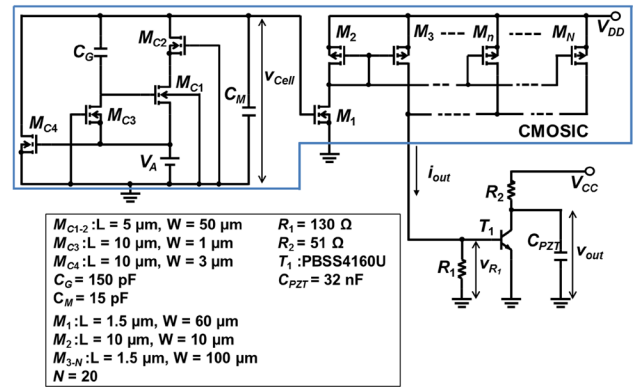**Fig. 7** Example of the output pulse waveform of the P-HNM (measured result)

Fig. 8 Frequency characteristic of a pulse-type hardware neuron model

(a) Circuit diagram

(b) Layout of FR4 circuit board

Fig. 9 The driving circuit for actuator
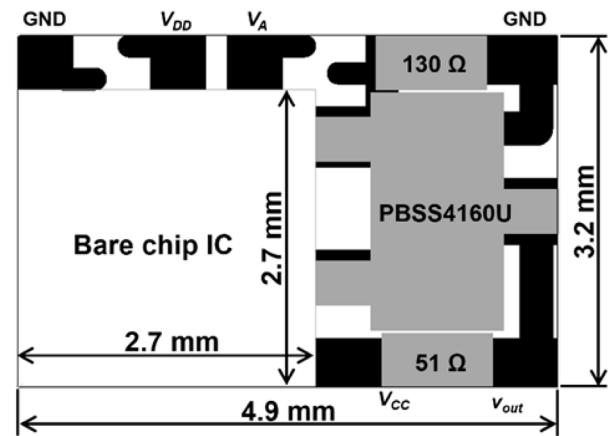
3.2 Output waveform of P-HNM

The example of output pulse waveform v_{Cell} of the P-HNM is shown in Figs. 6 and 7. Figure 6 shows a result of the simulation and Fig. 7 shows the measured result of the output pulse waveform of the constructed IC chip. The simulation result was given by HSPICE. The power supply voltage of the P-HNM was set to $V_A = 2.8$ V. Comparing the Figs. 6 and 7, oscillating frequencies are different (60 kHz in the simulation result, 17 kHz in the measured result). The piezoelectric element impact-type actuator can generate the rotational movement by a frequency from 10 to 50 kHz. Therefore, we apply the parasitic capacitance to the IC design.

3.3 Output waveform of current mirror circuit

The frequency characteristic of a pulse-type hardware neuron model is shown in Fig. 8. In the figure, the abscissa is frequency of P-HNM and the ordinate is output voltage. The value of power supply voltage V_A of the pulse-type hardware neuron model was $V_A = 2.2$ to 2.7 V in the simulation result, but it was $V_A = 2.6$–4.4 V in the measured

result. The power supply voltage of a current mirror circuit was $V_{DD} = 5.0$ V. The output voltage of the current mirror circuit is obtained as the voltage v_{R1} which is the voltage between both ends of the resistor $R_1 = 130$ Ω, which is shown in Fig. 9a.

3.4 Driving circuit of MEMS microrobot

The driving circuit of the piezoelectric element impact-type actuator consists of a bare chip IC of P-HNM with the current mirror circuit and the peripheral circuit. The peripheral circuit consists of a transistor and two resisters. Both bare chip IC and peripheral circuit is implemented on FR4 circuit board as shown in Fig. 9. The output of driving circuit was v_{out} as in Fig. 9a. The circuits with blue frame shown in Fig. 9a are constructed inside the bare chip IC. Circuit parameters of the peripheral circuit are resistor $R_1 = 130$ Ω and $R_2 = 51$ Ω. We used the transistor PBSS4160U (NXP Semiconductors, Inc.). The layout of the FR4 circuit board is shown in Fig. 9b. The size of the bare chip IC is 2.54 mm
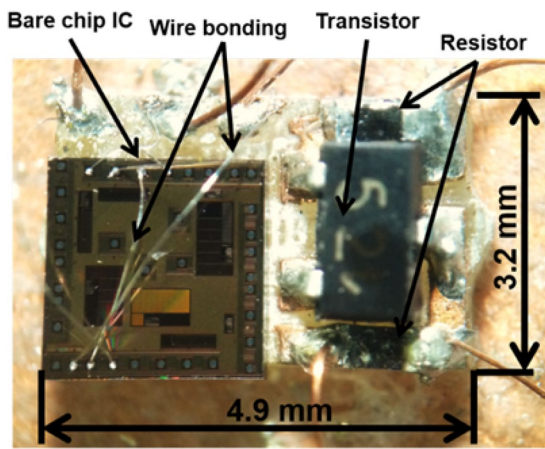
Fig. 10 Photograph of the fabricated driving circuit

Fig. 11 Frequency characteristics and peak to peak voltage characteristics vs. voltage source V_A

square in size. We construct the 2.7 mm square size groove to the FR4 circuit board.

Figure 10 shows the fabricated driving circuit. Wire bonding is used to connect the FR4 substrate with a bare chip IC. The size of the fabricated driving circuit is 3.2 mm × 4.9 mm, which can be mounted on the MEMS microrobot.

4 Rotational motion

4.1 Characteristics of the driving circuit

The characteristic of driving circuit is shown in Fig. 11. The abscissa shows V_A, and the ordinate shows frequency and peak to peak voltage of the voltage v_{out}. v_{out} is voltage between both ends of the capacitor C_{PZT}. The power supply voltage of the current mirror circuit and the transistor were set to $V_{DD} = 2.3$ V and $V_{CC} = 5.0$ V. In this figure, in the case of varying the V_A, the output frequency and the peak to peak voltage of output will change linearly.

4.2 Generation of rotational motion using driving circuit

Figure 12 shows the example of output waveform of the driving circuit. This output waveform allows the piezoelectric element impact-type actuator to rotate as shown in Fig. 13.

The driving circuit is connected to the piezoelectric element impact-type MEMS actuator, which generates the rotational motion. When the power supply voltage V_A of the P-HNM, the power supply voltage V_{DD} of a current mirror circuit, and the power supply voltage V_{CC} of a transistor were $V_A = 2.67$ V, $V_{DD} = 2.20$ V and $V_{CC} = 6.00$ V
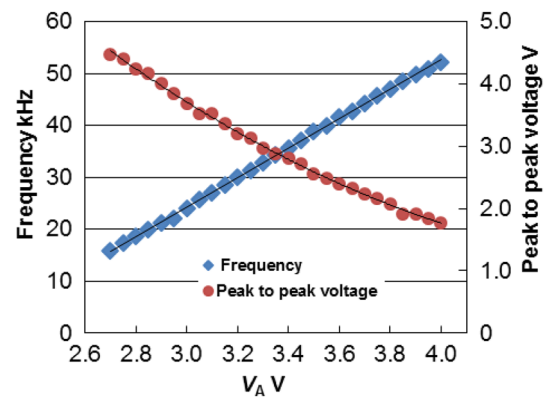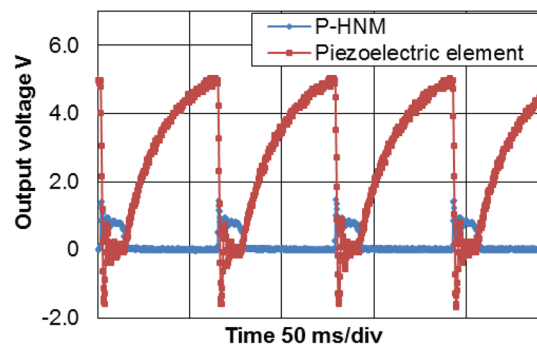

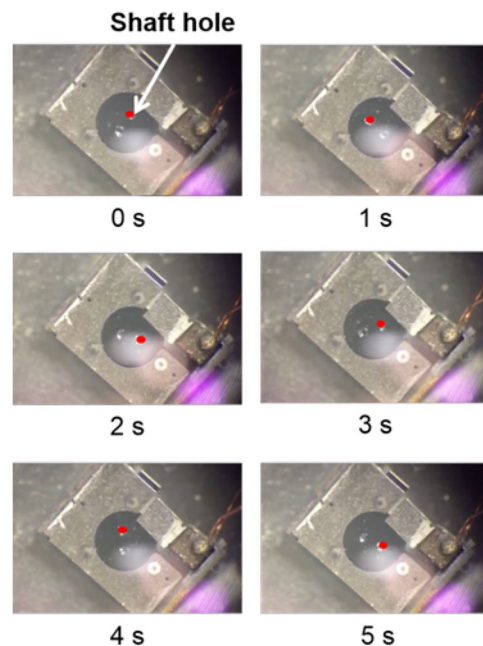Fig. 12 Output waveform of the driving circuit

Fig. 13 Rotational motion of the piezoelectric element impact-type MEMS actuator

respectively, the rotation of the rotor was obtained (Fig. 13). In Fig. 13, the rotor rotates at 24 rpm rotational motion.

As a result, our constructed driving circuit can actuate the actuator of the MEMS microrobot.

5 Conclusion

In this paper, we discussed the driving circuit which can generate the driving waveform of the piezoelectric element impact-type actuator. The driving circuit consists of the bare chip IC of the P-HNM using the CMOS process and the peripheral circuit. As a result, the following conclusions were drawn.

a) The bare chip IC of the P-HNM can be constructed with the CMOS technology.
b) The size of the driving circuit can be reduced to 3.2 mm × 4.9 mm, which allows it to be mounted on a MEMS microrobot.

In the future, we will construct the whole system of the piezoelectric element impact-type MEMS microrobot.

References

1. Shibata T, Aoki Y, Otsuka M et al (1997) Microwave energy transmission system for microrobot. IEICE Trans Electronics 80(2):303–308
2. Habib MK, Watanabe K, Izumi K (2007) Biomimetcs robot: from bio-inspiration to implementation. In: Proceedings of 33rd Annual Conference of the IEEE Industrial Electronics Society, pp143–148
3. Edqvist E, Snis N, Mohr RC et al (2009) Evaluation of building technology for mass producible millimeter-sized robots using flexible rinted circuitboards. J Micromech Microeng 19(7):11
4. Donald BR, Levey CG, McGray CD et al (2006) An untethered, electrostatic, globally controllable MEMS micro-robot. J Microelectromech Syst 15(1):1–15
5. Tai YC, Fan LS and Muller RS (1989) IC-processed micromotors: design, technology, and testing. Micro Electro Mechanical Systems. In: Proceedings, An Investigation of Micro Structure, Sensors, Actuators, Machines and Robots. IEEE, pp1–6
6. Mezaghi S, Koechli C, Perriard Y (2011) Development of a hybrid MEMS BLDC micromotor. IEEE Trans Ind Appl 47(1):3–11
7. Farahani AA, Suratgar AA and Taalebi HA (2013) Dynamics model and control of underwater fish-like micro mobile robot with PZT actuator. First RSI/ISM International Conference on Robotics and Mechatronics, pp 437–442
8. Iwata A, Amemiya Y (1995) Neural network LSI. IEICE, pp 1–2, pp 124–125
9. Lu Z, Ma S, Li B et al (2005) Design of a snake-like robot controller with cyclic inhibitory CPG model. In: IEEE International Conference on Robot and Biomimetics, pp 35–40
10. Hodgkin AL, Huxley AF (1952) A quanitative description of membrane current and its application to conduction and excitation in nerve. J Physiol 117(4):500–544
11. Nagumo J, Arimoto S, Yoshizawa S (1962) An active pulse transmission line simulating nerve axon. Proceedings of the IRE. 50:2061–2070
12. Sekine Y (1999) Pulse-type hardware neuron model. Computer today. 90:27–33, Saiens-sha Co. Ltd. Publishers
13. Sekine Y, Sumiyama M, Saeki K et al (2001) A Λ-type neuron model using enhancement-mode MOSFETs. IEICE, C, Vol. J84-C, No. 10, 988–994
14. Okazaki K, Ogiwara T, Yang D et al (2011) Development of pulse control type MEMS micro robot with hardware neural network. Artificial Life Robot 16:229–233
15. Uchikoba F, Takato M, Saito K (2012) Hardaware neural networks controlled MEMS rotational actuators and application to micro robot. J Mech Eng Automation 2:499–506
16. Maezumi K, Yamasaki S, Obara H et al (2014) Hexapod-Type SMA Driven MEMS Microrobot with Mounted Bare Chip Artificial Neural Networks IC. Proc Nineteenth Int Symp Artificial Life Robot 2014:401–405
17. Saito K, Matsuda A, Saeki K et al (2011) Synchronization of coupled pulse-type hardware neuron models for CPG model. The relevance of the time domain to neural network models, Springer Series on Cognitive and Neural Systems. pp 117–133